Heliyon 11 (2025) e40743

Contents lists available at ScienceDirect

Heliyon

journal homepage: www.cell.com/heliyon

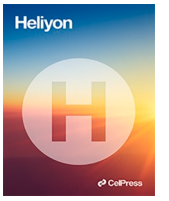

Research article

Effective removal of rhodamine B dyestuff using colemanite as an adsorbent: Isotherm, kinetic, thermodynamic analysis and mechanism

Feray Bayça

Alanya Alaaddin Keykubat University, Rafet Kayis Engineering Faculty, Department of Engineering Basic Science, 07450, Alanya, Antalya, Turkiye

ARTICLE INFO

Keywords:
Rhodamine B
Colemanite
Wastewater
Adsorption
Kinetic models
Isotherms

ABSTRACT

Removal of Rhodamine B (RhB) from aqueous solutions was performed by the batch adsorption process. Colemanite was characterized as an adsorbent by Fourier Transform Infrared Spectroscopy (FTIR), X-Ray Diffraction (XRD) and X-Ray Fluorescence (XRF). The effects of contact time, the effect of the initial concentration of the dye, the amount of adsorbent and temperature parameters on the removal of RhB were investigated. Equilibrium adsorption data of RhB on colemanite were analyzed using the Langmuir, Freundlich and Dubinin-Radushkevich isotherm models. It was found that the isotherm that showed the highest correlation with experimental data was the Langmuir isotherm. Using the Langmuir isotherm, the theoretical adsorption capacity was calculated as 42.02 mg/g. Adsorption kinetics were analyzed with Pseudo-First-Order, Pseudo-Second-Order and Intraparticle diffusion models. As a result of the calculations, it was determined that the most appropriate kinetic model was the Pseudo-Second-Order kinetic model. Thermodynamic studies have shown that adsorption is a physical, non-spontaneous, exothermic process in which randomness at the solid-liquid interface decreases. According to the results obtained, it can be said that colemanite can be used as a suitable adsorbent in the removal of Rhodamine B dye from wastewater.

1. Introduction

Wastes from many industries such as the textile, paper, chemistry, fertilizer, pesticide, metal plating, battery, food and medicine industries pose a significant threat to useable clean water resources [1]. In general, dyes block the penetration of sunlight into the water depths, increase the chemical oxygen demand of water and reduce the dissolved oxygen level. This causes the death of aquatic creatures and reduces water quality. It also causes bad odors in water [2].

RhB, a cationic dye, is the chloride salt of N-[9-(2-carboxyphenyl)-6-(diethylamino) 3H-xanthen-3-ylidene]-N-ethylethanaminium [3]. RhB is widely used in many industries, including the cosmetics, food, paper, leather and textile industries [4]. Since its aromatic rings have high physicochemical, thermal and optical stability, RhB is not completely degraded by general physicochemical and biological processes [5]. RhB is highly toxic and causes irritation in the eyes, skin and respiratory tract. Since the N-ethyl groups in the aromatic rings of RhB cause the dye to be highly toxic and carcinogenic, its use in the food and cosmetics industry is banned in many countries [6,7]. It is very important to remove RhB, which is so harmful to living things, from wastewater.

Different methods are applied to remove dyes from wastewater such as coagulation, ozonation, flocculation, chemical oxidation,

E-mail address: feray.bayca@alanya.edu.tr.

https://doi.org/10.1016/j.heliyon.2024.e40743
Received 4 September 2024; Received in revised form 21 November 2024; Accepted 26 November 2024
Available online 28 November 2024

ion exchange, reverse osmosis, photocatalysis, precipitation and adsorption [8,9]. Many of these methods have disadvantages such as high energy costs, complicated processes and the formation of undesirable by-products. However, adsorption is a highly preferred method because it is a cheap, easy and effective method [4,6]. Depending on the interactions between the adsorbent and the adsorbate, the adsorption process, that is retention of the adsorbate on the adsorbent surface, consists of three steps: (i) transport of dye molecules from the aqueous solution to the adsorbent surface, (ii) adsorption on to the adsorbent surface and (iii) desorption of dye molecules from the adsorbent surface to the aqueous medium [10].

There are studies in the literature of the use of different adsorbents to remove RhB from wastewater: kaolinite, montmorillonite [11], hypercrosslinked polymeric [12], raphiahookerie fruit epicarp [13], coffee grounds [14], banana peel [15], chitosan-pectin bio-adsorbent [16], pomegranate peel [4], and TiO_2-loaded chitosan biochar [17]. However, no study has been found in which colemanite was used as an adsorbent in the removal of RhB from wastewater.

The aim of this study was to remove Rhodamine B from wastewater using colemanite. For this purpose, the effects of the dosage amount of the adsorbent, the initial concentration of RhB, contact time and temperature parameters were investigated by working with the batch adsorption process. Using experimental data, the isotherm and kinetic models that best describe the adsorption were determined and thermodynamic parameters were calculated. The adsorption mechanism of RhB dye on colemanite was explained.

2. Material and method

In this study, cationic Rhodamine B (Isolab, Germany, 99 %) with molecular weight 479.01 g/mol and IUPAC name N-[9-(ortho-carboxyphenyl)-6-(diethylamino)-3H-xanthen-3-ylidene] diethyl ammonium chloride was used as the adsorbate. Ground colemanite ($Ca_2B_6O_{11}.5H_2O$) was obtained from Eti Mining (Turkiye). During the experimental studies, all solutions were prepared with ultrapure water. Calibration graphs were drawn with different concentrations of RhB dye at a wavelength of 554 nm using a UV–Vis spectrophotometer (Shimadzu, Japan).

In adsorption experiments, pH (4.6), stirring speed (400 rpm) and volume of RhB solution (50 mL) were kept constant, and the effects of adsorbent dosage (0.03–0.28 g), initial concentration of RhB (5–200 mg/L), solution temperature (25–60 °C) and contact time (5–240 min) were examined. At the end of adsorption, solid/liquid separation was carried out by centrifugation. The absorbance values of the liquid phase were measured. The equilibrium adsorption amount or adsorption capacity qe (mg/g) and the removal efficiency of RhB from aqueous solutions were calculated with Equation (1) and Equation (2) respectively.

$$\mathbf{q} = \frac{(\mathbf{C_o} - \mathbf{C_e})\,\mathbf{V}}{\mathbf{m}} \tag{1}$$

$$\mathbf{Removal\ efficiency} = \frac{(\mathbf{C_o} - \mathbf{C_e})}{\mathbf{C_o}}.\mathbf{100} \tag{2}$$

The properties of colemanite were examined using Rigaku ZSX a Primus II X-ray Fluorescence (XRF) spectrophotometer, PerkinElmer spectra BX 400 Fourier Transform Infrared Spectroscopy (FTIR), Quantachrome Autosorb-6 Brunauer-Emmett-Teller (BET), a Malvern laser particle sizer and Rigaku Ultima IV XRD. In the adsorption studies, a Shimadzu UV 1800 UV–VIS spectrophotometer and a Hanna model HI 221 pH meter were used.

3. Results and discussion

3.1. Characterization

In this study, characterization was performed by XRF, BET, FTIR and XRD analysis. Chemical analysis of the colemanite sample (except B_2O_3) was determined by XRF. The amount of B_2O_3 in the sample was determined by the volumetric method given in the literature [18].

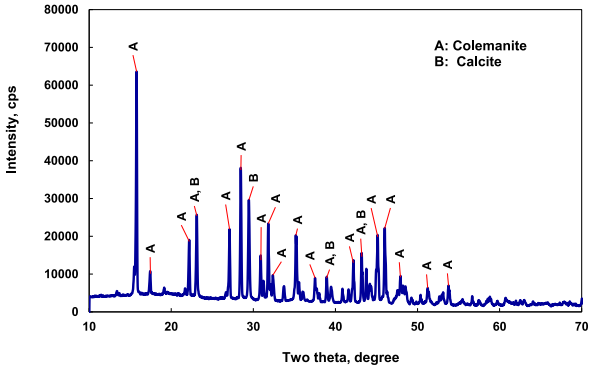

Fig. 1. XRD analysis of colemanite sample.

According to the chemical analysis results, the colemanite contained 42.69 % B_2O_3, 34.44 % CaO, 5.22 % SiO_2 and 2.90 % MgO. The mineral purity of the colemanite of this sample was calculated as 84.02 %. The BET surface area of the colemanite was measured as 10.12 m^2/g. The grain size of the colemanite with a sieve ratio of 90 % was measured as 72.30 μm.

Fig. 1 shows the XRD analysis results of ground colemanite. Strong peaks of 15.74° (020), 22.14° (021), 23.07° (210), 27.06° (22-1), 28.43° (031), 31.77° (040), 35.13° (022), 43.15° (051) and 45.11° (212) were observed in the crystal planes. These crystal planes and peak angles match well with JCPDS card number 01-074-2336, whose crystal planes belong to colemanite.

A few weak peaks were observed in crystal planes at 23.07° (012), 29.40° (104) and 35.96° (110). The angles and crystal planes at which these peaks are observed matched well with JCPDS card number 00-005-0586 to the calcite mineral. These XRD results indicate that the main mineral was colemanite and the minor mineral calcite.

3.2. Effect of adsorbent dosage

While investigating the effect of the amount of colemanite on the adsorption of RhB, the initial concentration of RhB (200 mg/L), stirring speed (400 rpm), solution pH (4.26) and time (60 min) were kept constant. The amount of colemanite was varied between 0.03 and 0.28 g/50 mL. In this study, the stirring speed was taken as 400 rpm. There are many studies in the literature on adsorption experiments being performed at a stirring speed of 400 rpm [19–24].

Fig. 2 shows the effect of adsorbent dosage on adsorption capacity and removal efficiency. It was observed that as the amount of adsorbent increased, the adsorption capacity decreased and the dye removal percentage increased. As the amount increases, the number of dye molecules per unit surface area of the adsorbent also increases. The empty active sites on the surface are filled more quickly and the adsorption capacity decreases over time, but as the amount of adsorbent increases, the surface area of the adsorbent increases, the amount of dye adsorbed on the unit surface increases and the removal percentage increases over time. In Fig. 2, as the amount of adsorbent goes from 0.03 g/50 mL to 0.28 g/50 mL, the adsorption capacity and removal percentage take decreasing values from 40.10 mg/g to 22.82 mg/g respectively, and reach 12.63 %. It is seen that the values increase from 1 to 64.19 %. Since the amount of adsorbent with which the highest adsorption capacity was obtained in equilibrium was 0.03 g/50 mL, this value was used when studying the effects of other parameters.

Li et al. [17] reported that the adsorption capacity of TiO_2-Loaded Chitosan biochar (TiO_2/CSB) decreased as the amount of adsorbent increased in the adsorption of RhB dye.

3.3. Effect of initial concentration of Rhodamine B

While examining the effect of the initial concentration (C_o) of RhB on adsorption, the amount of colemanite (0.03–0.28 g/50 mL), stirring speed (400 rpm), solution pH (4.26), time (60 min) and temperature (25 °C) were kept constant, and the initial concentration of RhB took values varying between 5 and 200 mg/L. Fig. 3 shows the effect of RhB initial concentration on adsorption capacity and removal efficiency. As a result of the experimental studies, it was found that as the initial concentration increased, the adsorption capacity increased but the removal percentage decreased. As the initial concentration increased from 5 mg/L to 200 mg/L, the adsorption capacities increased from 7.82 mg/g to 40.10 mg/g. On the other hand, removal efficiencies decreased from 93.85 % to 12.63 %. The highest adsorption capacity in equilibrium was reached at 200 mg/L. Therefore, 200 mg/L was chosen as the optimum initial concentration.

Ribeiro dos Santos et al. [25] stated that an increase in initial concentration accelerates the dye-colemanite interaction by increasing the number of dye molecules penetrating the colemanite surface per unit time and therefore increases the adsorption capacity.

3.4. Effect of contact time

The significance of contact time in the removal of RhB was optimized by working at different initial concentrations (5–200 mg/L) and different durations (5–240 min). During optimization, the amount of colemanite (0.03 g/50 mL), stirring speed (400 rpm),

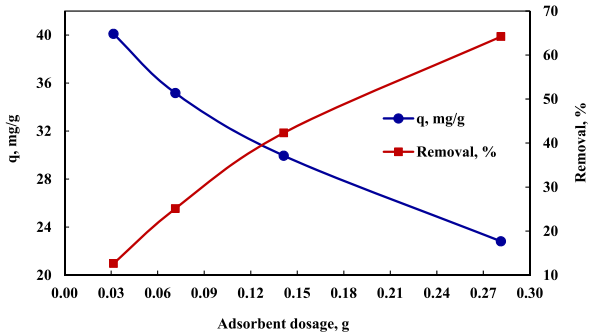

Fig. 2. Effect of adsorbent dosage on adsorption capacity and removal efficiency.

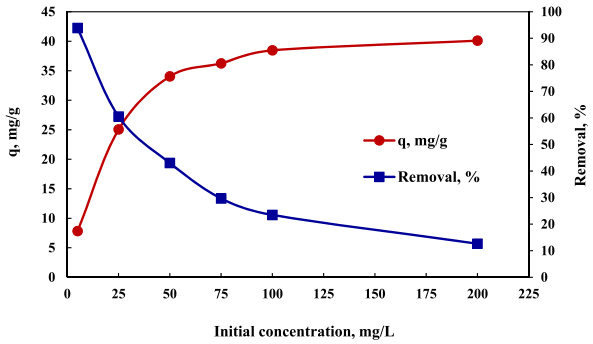

Fig. 3. Effect of RhB initial concentration on adsorption capacity and removal efficiency.

solution pH (4.26) and temperature (25 °C) were kept constant. The effect of contact time on adsorption capacity and removal efficiency is given in Fig. 4. It can be said that the system reaches equilibrium in 60 min and the adsorption capacity increases up to this point and remains constant after that. Over time, empty active sites on the adsorbent surface may reach saturation, causing the adsorption capacity to stabilize. Rahdar et al. [26] state that, while there are many sites for the adsorption of RhB on the adsorbent surface in the first minutes of adsorption, over time the number of RhB molecules in the surface and bulk phases becomes equal, and after this point, the adsorption capacity does not change since the adsorption and desorption rates will be equal to each other. Based on the equilibrium condition, the optimal contact time can be taken as 60 min.

3.5. *Effect of temperature*

In the temperature dependence study of adsorption, the initial concentration of RhB dye (200 mg/L), solution pH (4.26), stirring speed (400 rpm) and the amount of colemanite (0.03 g/50 mL) were taken as constant parameters, while adsorption experiments were conducted at solution temperature of 25–60 °C. Fig. 5 shows that the adsorption capacity decreases with increasing temperature. Therefore, it can be said that the adsorption process is exothermic. Adsorption capacities at temperatures of 25, 40 and 60 °C were found to be 41.35, 40.19 and 36.71 mg/g respectively. There are studies reporting a decrease of adsorption capacity with temperature [2,13].

3.6. *Modeling of adsorption isotherm*

The **Langmuir adsorption isotherm model** is defined as the monolayer and homogeneous adsorption of the adsorbate on the adsorbent surface. It emphasizes that the active sites on the adsorbent surface have equal affinity and surface energy towards the adsorbate molecules [27]. The mathematical Equation (3) for the Langmuir isotherm model is also included.

$$\frac{C_e}{q_e} = \frac{1}{K_L Q_m} + \frac{C_e}{Q_m} \tag{3}$$

Langmuir model parameters were calculated from the slope and the y axis intercept of the plot of C_e/q_e versus C_e. The dimensionless equilibrium parameter (R_L) is determined using Equation (4).

$$R_L = \frac{1}{1 + C_o K_L} \tag{4}$$

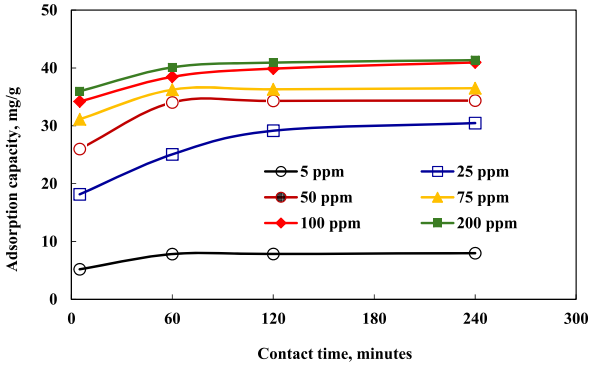

Fig. 4. Effect of contact time on adsorption capacity and removal efficiency.

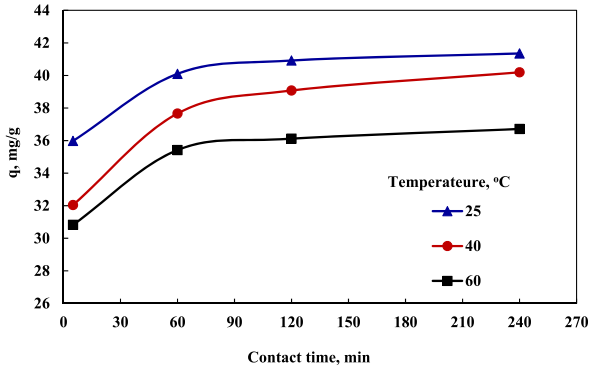

Fig. 5. Effect of temperature on adsorption capacity.

The dimensionless equilibrium parameter (R_L) calculated using Langmuir isotherm constants gives information about whether the adsorption process is irreversible ($R_L = 0$), favorable ($0 < R_L < 1$), linear ($R_L = 1$) or unfavorable ($R_L > 1$) [28].

The **Freundlich adsorption isotherm model** assumes that the adsorbent surface consists of heterogeneous active regions, and a multilayer adsorption occurs on the adsorbent surface [29]. The Freundlich isotherm is expressed as Equation (5) for linear adsorption.

$$\ln q_e = \ln Q_m + \frac{1}{n} \ln C_e \tag{5}$$

1/n in the range of 0.1–1.0 demonstrates good adsorption. The parameters 1/n and K_F were taken from the intercept and slope of the linear plot of '$\ln q_e$' versus '$\ln C_e$' of the Freundlich isotherm model [29].

The **Dubinin–Radushkevich (D–R) adsorption model** is an empirical model used to determine adsorption free energy and porosity. This model states that the adsorbent surface is heterogeneous and shows the Gaussian energy distribution of adsorption on heterogeneous regions. The D-R model is used to determine whether the adsorption process is physical or chemical [6]. The conformity of the experimental data to the linear form of the Dubinin-Radushkevich isotherm is determined using Equation (6).

$$\ln q_e = \ln Q_m + \beta.\varepsilon^2 \tag{6}$$

Polanyi potential was calculated with Equation (7).

$$\varepsilon = R\,T\left(1 + \frac{1}{C_e}\right) \tag{7}$$

If $E < 8$ kJ/mol, physical interactions are dominant in the adsorption process. If $8 < E < 16$ kJ/mol, adsorption occurs by ion exchange. If $E > 16$, the adsorption is chemical [6]. Adsorption energy (E) was calculated using Equation (8).

$$E = \frac{1}{\sqrt{-2\beta}} \tag{8}$$

In this study, the maximum adsorption capacities and isotherm constants calculated by applying the obtained experimental data to each adsorption isotherm model are given in Table 1, and Fig. 6 shows adsorption isotherm models for RhB on colemanite of a) the Langmuir isotherm, b) the Freunlich isotherm and c) the Dubinin-Radushkevich isotherm. R^2 values of the Langmuir, Freunlich and Dubinin–Radushkevich isotherms were found to be 0.9981, 0.9127 and 0.9692 respectively. When R^2 values are compared, it is clear that the highest correlation coefficient is obtained in the Langmuir isotherm model. Therefore, we can describe the adsorption of RhB dye on colemanite by the Langmuir isotherm.

Table 1
Parameters of adsorption isotherm models of RhB on natural colemanite.

Linear isotherm	Parameters	Values
Langmuir	$Q_{m,\,cal.}$ (mg/g)	42.02
	R_L	0.019
	K_L (L/mg)	0.264
	R^2	0.9981
Freundlich	$Q_{m,\,cal.}$ (mg/g)	13.87
	1/n	0.2499
	R^2	0.9127
Dubinin - Radushkevich	$Q_{m,\,cal.}$ (mg/g)	36.58
	β	0.17
	E (kJ/mol)	2.41
	R^2	0.9692

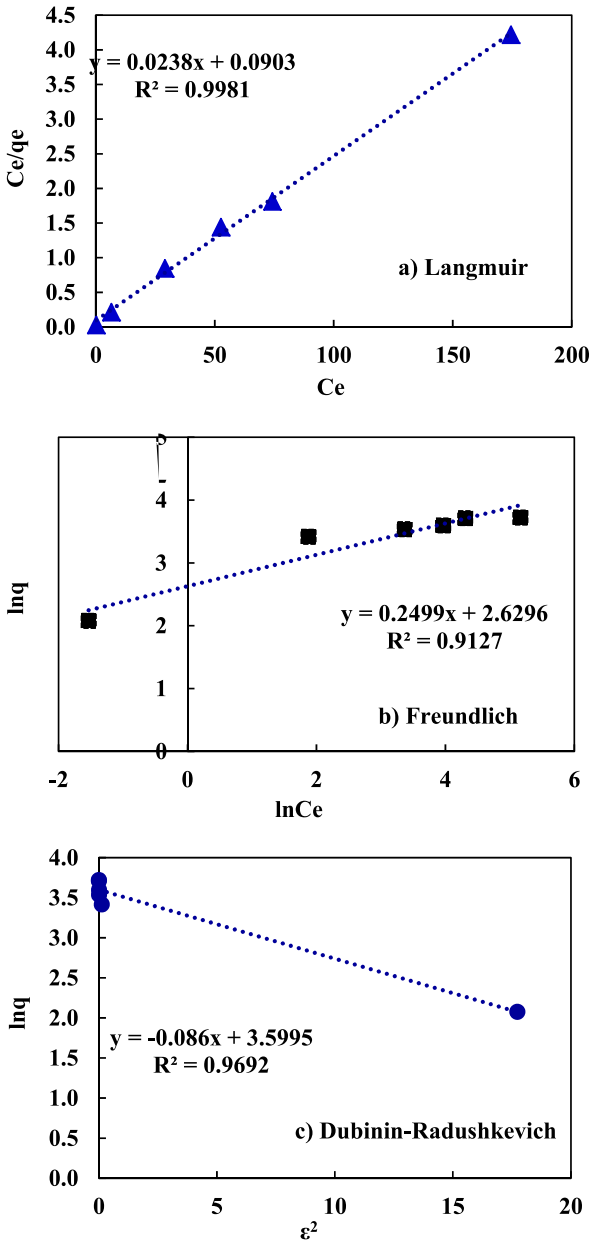

Fig. 6. Adsorption isotherm models for RhB on colemanite of the **a)** Langmuir isotherm, **b)** Freunlich isotherm and **c)** Dubinin-Radushkevich isotherm.

3.7. Chi-square statistical analysis of isotherm models

Chi-square statistical analysis is an analysis that shows how close the adsorption capacity calculated from the adsorption isotherm model is to the experimental adsorption capacity value. In other words, Chi-square statistical analysis is an error analysis. The lower the Chi-square value, the lower the error. In this analysis, the isotherm model with the χ^2 value closest to zero is the most suitable adsorption model. Chi-square values were calculated by using Equation (9).

$$\chi^2 = \sum_{i=1}^{n} \frac{\left(q_{exp} - q_{cal}\right)^2}{q_{exp}} \tag{9}$$

Here q_{exp} is the experimental adsorption capacity (mg/g), and q_{cal} is the adsorption capacity calculated from the isotherm model (mg/g). In this study, isotherm models were examined by performing Chi-square analysis in order to verify the most appropriate isotherm

describing the adsorption system, and the results are given in Table 2.

The χ^2 values calculated for the Langmuir isotherm model, Freundlich isotherm model and Dubinin-Radushkevich (D-R) isotherm were 0.011, 18.260 and 0.550, respectively. When χ^2 values are compared, it can be said that the model that best describes the system is the Langmuir isotherm model. Although the χ^2 value of the D-R isotherm model and the χ^2 value of the Langmuir isotherm model are close to zero, the R^2 value of the Langmuir isotherm model is considerably larger than the R^2 value of the Dubinin-Radushkevich (D-R) isotherm model. Based on this, the most suitable isotherm model according to statistical chi-square analysis is the Langmuir isotherm. In addition, the fact that the experimental adsorption capacity (q_{exp}, 41.35 mg/g) and the theoretical adsorption capacity (Q_m, 42.02 mg/g) are very close to each other is another indicator that supports the Langmuir isotherm as the most suitable isotherm.

There are studies in the literature in which the adsorption of RhB with different adsorbents fits the Langmuir isotherm model [8, 30–33]. Table 3 shows the comparison between this study and studies in the literature in terms of maximum adsorption capacities. As a result of the comparisons, it can be said that colemanite can be used as a potential adsorbent in the removal of RhB dye from wastewater.

In this study, the maximum adsorption capacity for the removal of RhB dye with colemanite was found to be 42.02 mg/g. In the literature, maximum adsorption capacities for the adsorption of RhB ranging from 3 to 161 mg/g have been found.

3.8. Determination of adsorption kinetic model

In order to determine the most suitable kinetic model for the adsorption of RhB dye on colemanite, the adsorption mechanism and rate determining step were determined by applying the experimental data to the Langregren or pseudo first order (PFO) model and the pseudo second order (PSO) and Intra-particle diffusion (IpD) models. The correlation coefficients obtained from each kinetic model and the coefficients of the model are listed in Table 4.

The mathematical expression of the pseudo first order kinetic model, known as the Langregren equation, is given in Equation (10). q_e was calculated from the slope of the graph and the intersection of the y-axis K_1.

$$\mathbf{ln(q_e - q_t) = ln\ q_e - K_1\ t} \tag{10}$$

The mathematical equation of the pseudo second order kinetic model is given in Equation (11). q_e is calculated from the slope of the graph and K_2 is calculated from the y-axis intersection [34].

$$\frac{\mathbf{t}}{\mathbf{q_t}} = \frac{\mathbf{1}}{\mathbf{K_2 \bullet q_e^2}} + \frac{\mathbf{t}}{\mathbf{q_e}} \tag{11}$$

The intraparticle diffusion model, formulated from the Weber and Morris model, is another kinetic model used to determine the rate-determining step of the adsorption process. In an adsorption process, the dye in solution is transported to the adsorbent surface by mass transfers such as surface diffusion, film diffusion and pore diffusion. The IpD model allows it to be learned whether adsorption is diffusion controlled. The mathematical expression of the intra-particle diffusion model is given in Equation (12). If the rate controlling step is intra-particle diffusion, the $q_t = f\ (t^{1/2})$ graph gives a linear graph [33].

$$\mathbf{q_t = K_p . t^{1/2} + C} \tag{12}$$

When determining the kinetic model in an adsorption process, the correlation coefficients of each graph drawn by applying experimental data to different kinetic models must be close to one (R^2) and the theoretical (q_{cal}, mg/g) and experimental (q_{exp}, mg/g) adsorption capacities must be close to each other. While making a kinetic analysis of the adsorption of RhB dye on colemanite, the amount of colemanite (0.03 g/50 mL), stirring speed (400 rpm), solution pH (4.26) and temperature (25 °C) were kept constant. Meanwhile, kinetic calculations were made using different initial concentrations of RhB dye (5–200 mg/L) and the adsorption capacities obtained at each concentration point in the 5–240 min interval. Parameters of adsorption kinetic models and maximum adsorption capacity (Q_{max}) of RhB on colemanite are given in Table 4.

Considering the correlation coefficients (R^2) of the kinetic models, the R^2 values of the PFO and IpD kinetic models are quite low. The q_{cal} and q_{exp} values in the models in question are not close to each other. These results prove that neither the PFO nor the IpD models are kinetic models that describe adsorption. Since the R^2 value of the PSO model is close to one and the theoretical (q_{cal}, mg/g) and experimental (q_{exp}, mg/g) adsorption capacities calculated for each initial concentration in the PSO model are close to each other, it can be said that the kinetic model sought is PSO. In the PSO kinetic model, the theoretical adsorption capacity (q_{cal}) was calculated as 41.49 mg/g and the experimental adsorption capacity (q_{exp}) was calculated as 41.35 mg/g at 200 mg/L, where the highest adsorption capacity was obtained. There are studies in the literature where the adsorption kinetic model of RhB dye fits the PSO model [31,35,36]. PSO kinetic model graphs for RhB onto colemanite are given in Fig. 7.

Table 2
R^2 and chi-square (χ^2) values of adsorption isotherm models of RhB on colemanite.

Isotherm models	R^2	χ^2
Langmuir isotherm	0.9981	0.011
Freundlich isotherm	0.9127	18.260
Dubinin-Radushkevich isotherm	0.9692	0.550

Table 3
Comparison of maximum adsorption capacities of different adsorbents in the removal of RhB dye from aqueous solutions.

Adsorbent	Isotherm	Q_{max}, mg/g	References
Modifying Fe_3O_4 nanoparticles	Langmuir	161	[30]
Nanoscaled ZnO	Freundlich	97	[8]
Natural colemanite	Langmuir	42	This study
Eichhornia crassipes	Langmuir	27	[31]
Almond shell	Langmuir	14	[9]
Ferromagnetic $BiFeO_3$	Langmuir	12	[45]
Natural diatomite	Freundlich	10	[32]
Expanded Perlite	Langmuir	3	[33]

Table 4
Parameters of adsorption kinetic models and maximum adsorption capacity of RhB on natural colemanite.

C_o	Qe	Pseudo First order			Pseudo Second order			Intraparticle Diffusion		
	exp	(PFO)			(PSO)			(InP)		
mg/L	mg/g	Qe mg/g	K_1	R^2	Qe mg/g	K_2	R^2	C mg/g	K_{id} mg/g.mi	R^2
5	7.97	0.98	-3E-03	0.7562	**8.05**	0.0487	1.0000	**5.34**	0.205	0.7193
25	30.47	14.79	-8E-05	0.9842	**31.35**	0.0037	0.9977	**15.92**	0.973	0.9350
50	34.36	7.79	-2E-04	0.9423	**34.60**	0.0232	1.0000	**26.52**	0.703	0.7027
75	36.50	3.71	-1E-04	0.7911	**36.63**	0.0334	1.0000	**31.45**	0.395	0.7119
100	40.96	7.03	-7E-05	0.9946	**41.32**	0.0084	0.9997	**33.70**	0.513	0.9305
200	41.35	5.49	-9E-05	0.9867	**41.49**	0.0163	1.0000	**35.89**	0.406	0.8442

3.9. Thermodynamic parameters

Thermodynamic parameters related to adsorption provide information about whether the adsorption process is endothermic or exothermic, whether it is spontaneous or not, and the disorder of the system [26]. Enthalpy change (ΔH^o), entropy change (ΔS^o) and Gibbs free energy change (ΔG^o) are the thermodynamic parameters that define the system. equations (13)–(15) that enable the calculation of these parameters are given below.

$$\mathbf{\Delta G^o = \Delta H^o - T.\Delta S^o} \tag{13}$$

$$\mathbf{\Delta G^o = -R.T.InK_d} \tag{14}$$

$$\mathbf{In\ K_d = \frac{\Delta S^o}{R} - \frac{\Delta H^o}{R.T}} \quad \mathbf{(Van't\ Hoff\ plot)} \tag{15}$$

The values of ΔH^o and ΔS^o are obtained from the slope and intercept of the plot between In K_d and 1/T (Van't Hoff plot). Adsorption experiments were carried out at 25, 40 and 60 °C to determine the thermodynamic parameters. The plot of the Van't Hoff equation (ln K_d versus 1/T) calculation of thermodynamic parameters for the adsorption of methylene blue on to colemanite is given in Fig. 8. Calculated thermodynamic parameters for the adsorption of RhB are listed in Table 5. It can be seen that all the Gibbs free energy change (ΔG^o) values are positive and increase with increasing temperature. The Gibbs free energy change at 25, 40 and 60 °C are calculated as 3.65, 4.01 and 4.46 kJ/mol, respectively. These positive ΔG^o values indicate that the adsorption process of RhB onto colemanite is not spontaneous.

In this study, the enthalpy change (ΔH^o) found for the adsorption of RhB dye on colemanite is −3.29 kJ/mol. Since the enthalpy change is negative, this adsorption process is an exothermic reaction. Azeez et al. [2], Postai et al. [37] and Elmoubarki et al. [38] reported that negative entropy indicates that the disorder at the solid-liquid interface decreases in adsorption.

The entropy change (ΔS^o) for the adsorption of RhB dye on colemanite was found to be −23.28 J/mol.K. Since the entropy change is negative, this adsorption process can be attributed to the low affinity of colemanite for RhB molecules. Similar results were found in other studies [4,14].

3.10. Adsorption mechanism of Rhodamine-B on colemanite

The effect of pH on the zeta potentials of the colemanite is given in Fig. 9. The zeta potential of the colemanite mineral has a negative surface charge between pH = 2.2 and 11.1. Furthermore, the surface charge of colemanite was found to be −9 mV at pH = 2.2 and −21 mV at pH = 11.1 [39].

In this study, the pH of RhB solutions was kept constant at 4.25. At pH = 4.25, the surface charge of colemanite will be negative. Since the affinity of the positively charged RhB dye to the negatively charged colemanite will be high at pH = 4.25, it can be said that there will be a strong electrostatic interaction between RhB and colemanite.

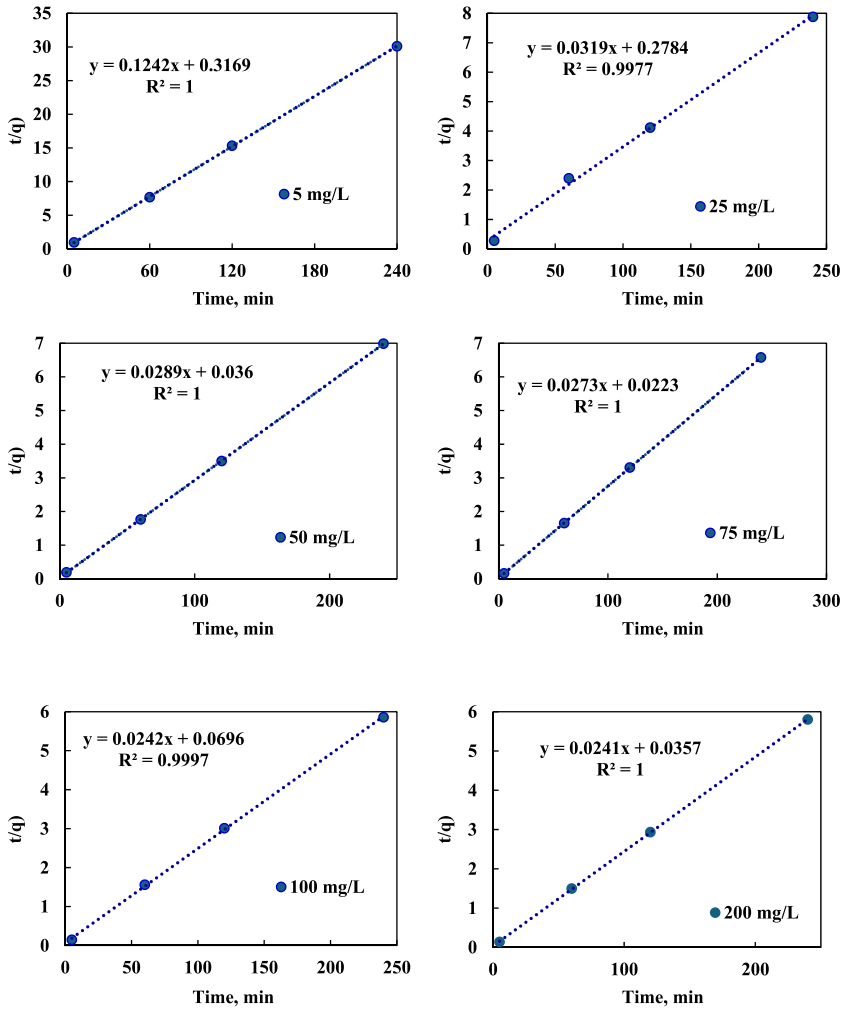

Fig. 7. Pseudo second order kinetic model graphs for RhB on to colemanite.

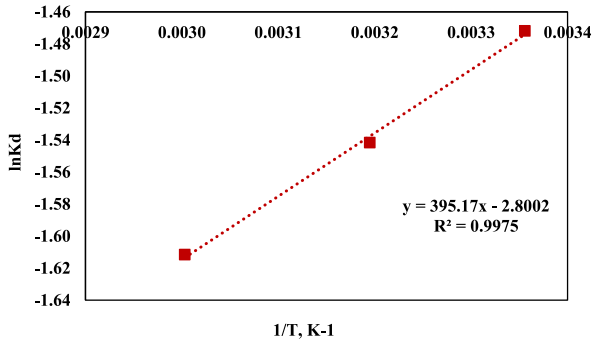

Fig. 8. Plot of Van't Hoff equation (ln K_d versus 1/T) calculation of thermodynamic parameters.

The mechanism of adsorption of RhB on colemanite is given in Fig. 10. Colemanite is negatively charged and RhB is positively charged. With the help of van der Waals interaction, it forms a complex that reduces the repulsive forces of oppositely charged adsorbent-adsorbate, This complex reduces the hydrophobic interactions and van der Waals interactions between the same charged dye particles. Pal et al. [40] reported that the interaction of dye particles with the aqueous medium becomes easier with the decrease in hydrophobicity.

In Fig. 10, the three coordinated boron atoms (B_3) in colemanite act as acceptors because their p_z orbitals are empty. RhB, on the

Table 5
Thermodynamic parameters of adsorption of RhB on to natural colemanite.

Temperature K	ΔG° kJ/mol	ΔH° kJ/mol	ΔS° J/mol.K	R^2
298	3.65	−3.29	−23.28	0.9975
313	4.01			
333	4.46			

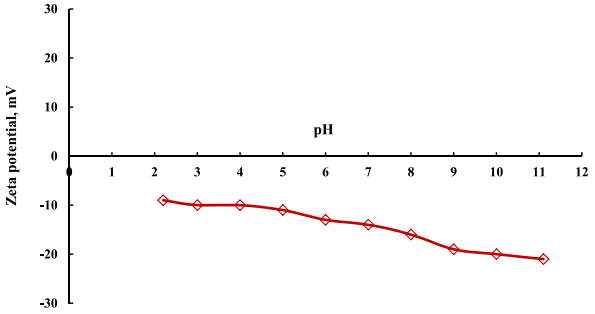

Fig. 9. Effect of pH on the zeta potentials of the colemanite [39].

other hand, carries aromatic rings with an electron-rich π electron system. These rings act as donors. Strong intermolecular bonds can be established through the π-p_z interaction formed between three coordinated boron atoms and aromatic rings. The negatively charged oxygen (-O-) attached to the four coordinated boron atoms (B_4) in colemanite can interact electrostatically with the positively charged nitrogen atom ($+N^{-1}$) in the RhB molecule [41]. -B-O-B- bonds, which act as bridges between the two B_2O_3 hexagonal rings in colemanite, can increase the electronegativity of colemanite, strengthening the electrostatic interaction with RhB and increasing adsorption [39], and hydrogen bonds can be established between the nitrogen (N) atom in the amine group in RhB and the OH group attached to the four coordinated boron atoms in colemanite [41].

It was determined that the adsorption of RhB dye on colemanite obeyed the pseudo second order (PSO) kinetic model and was described by the Langmuir adsorption isotherm. The PSO kinetic model can be attributed to chemisorption [42]. The Langmuir isotherm can indicate that adsorption can occur chemically and in a single layer. However, determining kinetic and isotherm models may not be fully sufficient to elucidate the adsorption mechanism. For this purpose, changes in chemical bonds due to adsorbent-adsorbate interaction during adsorption were determined by FTIR analysis. FTIR spectra of colemanite before and after adsorption are given in Figs. 11 and 12.

Table 6 shows FTIR data before and after adsorption of RhB onto colemanite. The -OH groups found in water molecules give peaks in the IR region in the range of 3250–3600 cm^{-1}. It was observed that the -OH groups in colemanite gave peaks in similar places both before adsorption (3212.50 cm^{-1}) and after adsorption (3220.59 cm^{-1}). At this point, the shifts in the frequencies of water molecules before and after are insignificant in terms of the adsorption of RhB on the adsorbent surface. The peak shifts of -OH groups do not support the adsorption of the dye.

However, the tensile deformation of H–O–H bonds in the FTIR of colemanite before adsorption belongs to the peak seen at 2106.75 cm^{-1}. After adsorption, this peak shifted to 2339.47 cm^{-1}. This shows that the dye is retained on the surface. While the symmetric stretching vibration of the B_3–O bond was observed at 1118.60 cm^{-1} before adsorption, the same peak shifted to 1131.98 cm^{-1} after adsorption. The symmetric stretching of the B_3–O bond which was observed at 1014.41 cm^{-1} before, shifted to 1002.8 cm^{-1} afterwards. Symmetric stretching vibration of the B_4 – O bond was 758.97 before adsorption and 728.36 cm^{-1}.

The stretching vibration of the C = O bond in the carbonyl group of the carboxyl group is observed at 1641.23 cm^{-1} and the vibration of the Ar – C bond is observed at 1317.23 cm^{-1}. These peaks show that the RhB dye is adsorbed on the colemanite surface.

In adsorption studies with colemanite in the literature, stretching vibrations of the O–H bond in colemanite are observed at frequencies of 3603 cm^{-1} [39], in the band range of 3310–3235 cm^{-1} [43], at frequencies of 3326.91 and 3609.50 cm^{-1} [44] and in the 3189–3727 cm^{-1} band range [46]. Symmetric stretching vibrations of B_3 – O and B_4 – O bonds in colemanite are at 916.29 cm^{-1} and 655 cm^{-1} [44], and 882 and 756 7 cm^{-1} [36] and 762.14 cm^{-1} [44]. In various studies, the bending vibration of the B–O–H bond was measured at 1224.57 cm^{-1} [44], at 1315 and 1228 cm^{-1} [46], and at 812 cm^{-1} [43].

When the data are combined, due to the displacement of the characteristic peaks in colemanite, it can be said that RhB is adsorbed on colemanite.

4. Conclusions

In this study, Rhodamine B (RhB), a cationic dye, was removed from aqueous solutions by the adsorption method using natural colemanite as an adsorbent. Based on both the R^2 values of the adsorption isotherm models and the statistical chi-square (χ^2) analysis, it was determined that the Langmuir isotherm model was the most suitable for RhB adsorption on to colemanite. The maximum

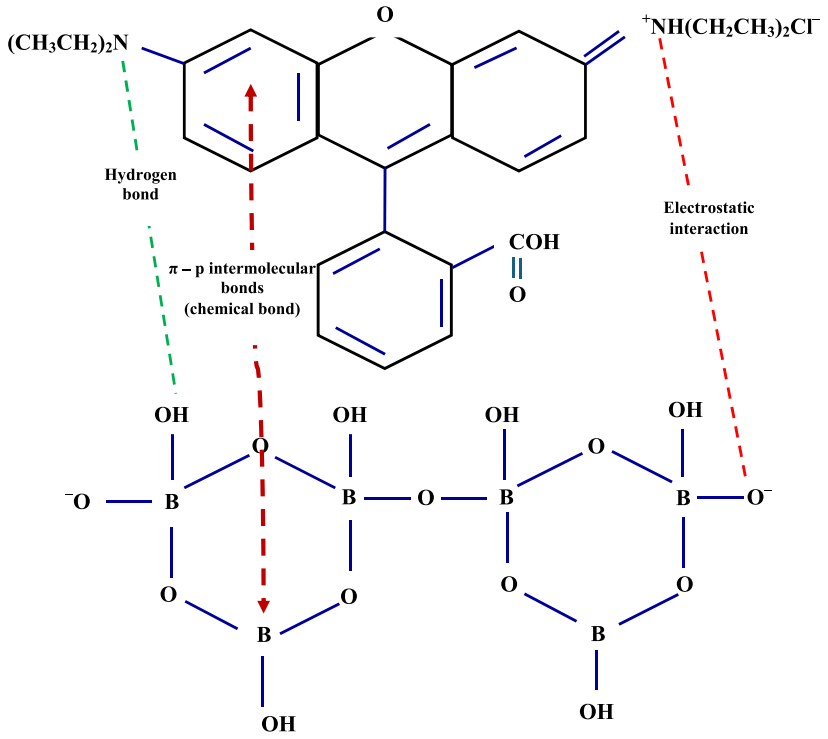

Fig. 10. Adsorption mechanism of RhB on colemanite.

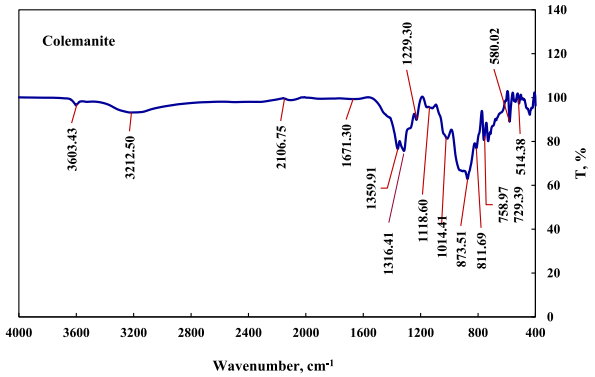

Fig. 11. FTIR spectrum of natural colemanite before adsorption.

adsorption capacity value of 42.02 mg/g calculated for the Langmuir isotherm model is very close to the value of 41.35 mg/g found for the experimental adsorption capacity. A removal efficiency of 95 % was achieved at low RhB concentrations. Pseudo-first-order model, pseudo-second-order model and intraparticle kinetic models were analyzed using experimental data. The pseudo-second-order kinetic model best described the adsorption of RhB dye on natural colemanite. As the amount of adsorbent increased, the adsorption capacity decreased and the dye removal percentage increased. The q_e value increased slowly with increasing contact time. As the temperature increased, the adsorption capacity decreased. Therefore, the adsorption process can be conducted successfully at room temperature. Thermodynamic studies have determined that the adsorption process is exothermic and not chemically spontaneous. It has been shown that the randomness at the solid-liquid interface decreases in the adsorption process. As a result of both the Dubinin–Radushkevich isotherm and thermodynamic calculations, it was determined that the adsorption process of RhB dye on natural colemanite was controlled by physical adsorption. The adsorption mechanism can be explained as adsorption occurring due to the electrostatic attraction between the positively charged RhB dyestuff and the negatively charged surface-charged colemanite. This is attributed to a physical adsorption process between RhB and colemanite. It can be explained that the adsorption of negatively charged colemanite and positively charged RhB cation occurs due to electrostatic attraction forces. Natural colemanite can be a successful and inexpensive

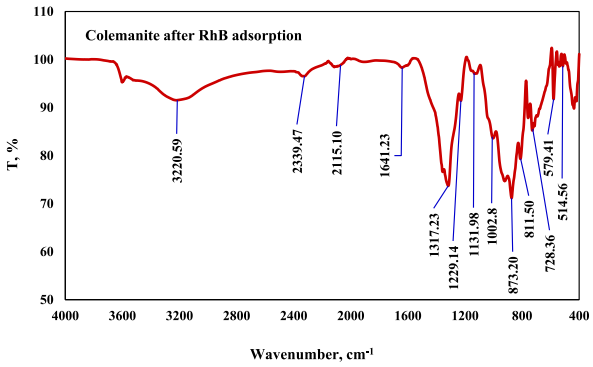

Fig. 12. FTIR spectrum of colemanite after RhB adsorption.

Table 6
FTIR data before and after adsorption of RhB onto colemanite.

Vibrations in bonds	Before adsorption	After adsorption
O-H bond in H_2O	3212.50	3220.59
Stretching deformation of H-O-H bond	2106.75	2339.47
Symmetric stretching vibration in B_3-O bond	1118.60	1131.98
Symmetric stretching of the B_3-O bond	1014.41	1002.8
Symmetric stretching vibrations of the B_4-O bond	758.97	728.36

adsorbent in the treatment of wastewater containing RhB dyes. Since RhB is carcinogenic, its use in coloring food and cosmetics is banned in many countries.

Data availability statement

The authors do not have permission to share data.

Ethics declaration

This study does not involve any human or animal testing.

Funding

The author declares they have no financial interests.

Declaration of competing interest

The authors declare that they have no known competing financial interests or personal relationships that could have appeared to influence the work reported in this paper.

References

[1] R. Gusain, K. Gupta, P. Joshi, O.P. Khatri, Adsorptive removal and photocatalytic degradation of organic pollutants using metal oxides and their composites: a comprehensive review, Adv. Colloid Interface Sci. 272 (2019) 102009.
[2] L. Azeez, A. Lateef, S.A. Adebisi, A.O. Oyedeji, Novel biosynthesized silver nanoparticles from cobweb as adsorbent for Rhodamine B: equilibrium isotherm, kinetic and thermodynamic studies, Appl. Water Sci. 8 (2018) 1–12.
[3] W. Begum, B. Saha, U. Mandal, Characterization of saponin extracted from Acacia concinna (shikakai or soap pod) and thermodynamic studies of its interaction with organic dye rhodamine B, Chemistry Africa 7 (2024) 2539–2552.
[4] R. Ghibate, O. Senhaji, R. Taouil, Kinetic and thermodynamic approaches on Rhodamine B adsorption onto pomegranate peel, Case Studies in Chemical and Environmental Engineering 3 (2021) 100078.
[5] A.I. Adeogun, R.B. Balakrishnan, Kinetics, isothermal and thermodynamics studies of electrocoagulation removal of basic dye Rhodamine B from aqueous solution using steel electrodes, Appl. Water Sci. 7 (2017) 1711–1723.
[6] J. Sahar, A. Naeema, M. Farooqa, S. Zareena, A. urRahmanb, Thermodynamic studies of adsorption of rhodamine B and Congo red on graphene oxide, Desalination Water Treat. 164 (2019) 228–239.
[7] A.A. Hakami, S.M. Wabaidur, M.A. Khan, Z.A. AlOthman, M.R. Siddiqui, Extraction procedures and analytical methods for the determination of methylene blue, rhodamine B and crystal violet-an overview, Curr. Anal. Chem. 17 (2021) 708–728.
[8] J. Godwin, J.R. Njimou, N. Abdus-Salam, P.K. Panda, B.C. Tripathy, M.K. Ghosh, S. Basu, Nanoscale ZnO-adsorbent carefully designed for the kinetic and thermodynamic studies of Rhodamine B, Inorg. Chem. Commun. 138 (2022) 109287.

[9] Z.M. Şenol, N.E. Messaoudi, Y. Fernine, Z.S. Keskin, Bioremoval of rhodamine B dye from aqueous solution by using agricultural solid waste (almond shell): experimental and DFT modeling studies, Biomass Conversion and Biorefinery (2023) 1–14.
[10] S.H. Teo, C.H. Ng, A. Islam, G. Abdulkareem-Alsultan, C.G. Joseph, J. Janaun, Y.H. Taufiq-Yap, S. Khandaker, G.J. Islam, H. Znad, M.R. Awual, Sustainable toxic dyes removal with advanced materials for clean water production: a comprehensive review, J. Clean. Prod. 332 (2022) 130039.
[11] K.G. Bhattacharyya, S. SenGupta, G.K. Sarma, Interactions of the dye, rhodamine B with kaolinite and montmorillonite in water, Appl. Clay Sci. 99 (2014) 7–17.
[12] J.H. Huang, K.L. Huang, S.Q. Liu, A.T. Wang, C. Yan, Adsorption of Rhodamine B and methyl orange on a hypercrosslinked polymeric adsorbent in aqueous solution, Colloids Surf. A Physicochem. Eng. Asp. 330 (2008) 55–61.
[13] A.A. Inyinbor, F.A. Adekola, G.A. Olatunji, Adsorption of Rhodamine B dye from aqueous solution on Irvingia gabonensis biomass: kinetics and thermodynamics studies, S. Afr. J. Chem. Eng. 68 (2015) 115–125.
[14] K. Shen, M.A. Gondal, Removal of hazardous Rhodamine dye from water by adsorption onto exhausted coffee ground, J. Saudi Chem. Soc. 21 (2017) S120–S127.
[15] A.A. Oyekanmi, A. Ahmad, K. Hossain, M. Rafatullah, Statistical optimization for adsorption of Rhodamine B dye from aqueous solutions, J. Mol. Liq. 281 (2019) 48–58.
[16] A. Mohrazi, R. Ghasemi-Fasaei, Removal of methylene blue dye from aqueous solution using an efficient chitosan-pectin bio-adsorbent: kinetics and isotherm studies, Environ. Monit. Assess. 195 (2023) 339.
[17] X.F. Li, R.X. Li, D.S. He, X.Q. Feng, Superior adsorption performance of TiO_2-loaded chitosan biochar for rhodamine B dye, Russ. J. Inorg. Chem. 68 (2023) 1084–1095.
[18] S.U. Bayca, Microwave radiation leaching of colemanite in sulfuric acid solutions, Separation and Purification Technology 105 (2013) 24–32.
[19] C.A. Basar, Applicability of the various adsorption models of three dyes adsorption onto activated carbon prepared waste apricot, J. Hazard Mater. B135 (2006) 232–241.
[20] S.M. Ramraj, A. Kubaib, P.M. Imran, M.K. Thirupathy, Utilizing Sida Acuta leaves for low-cost adsorption of chromium (VI) heavy metal with activated charcoal, Journal of Hazardous Materials Advances 11 (2023) 100338.
[21] M. Cuccarese, S. Brutti, A. De Bonis, R. Teghil, F. Di Capua, I.M. Mancini, S. Masi, D. Caniani, Sustainable adsorbent material prepared by soft alkaline activation of spent coffee grounds: characterisation and adsorption mechanism of methylene blue from aqueous solutions, Sustainability 15 (2023) 2454.
[22] B. Rzig, R. Kojok, E.B. Khalifa, G. Magnacca, T. Lahssini, B. Hamrouni, N. Bellakhal, Adsorption performance of tartrazine dye from wastewater by raw and modified biomaterial: equilibrium, isotherms, kinetics and regeneration studies, Biomass Conversion and Biorefinery 14 (2024) 18313–18330.
[23] T.S. Hamidon, M.H. Hussin, Improved p-chlorophenol adsorption onto copper-modified cellulose nanocrystal-based hydrogel spheres, Int. J. Biol. Macromol. 233 (2023) 123535.
[24] F. Rouhani, P. Mousavifard, Tenfold increase in adsorption capacity of HKUST-1 toward Congo red by producing defective MOF under controlled thermal treatment, Separation and Purification Technology 320 (2023) 124230.
[25] F. Ribeiro dos Santos, H.C. de Oliveira Bruno, L. Zelayaran Melgar, Use of bentonite calcined clay as an adsorbent: equilibrium and thermodynamic study of Rhodamine B adsorption in aqueous solution, Environ. Sci. Pollut. Control Ser. 26 (2019) 28622–28632.
[26] S. Rahdar, A. Rahdar, M.N. Zafar, S.S. Shafqat, S. Ahmadi, Synthesis and characterization of MgO supported Fe–Co–Mn nanoparticles with exceptionally high adsorption capacity for Rhodamine B dye, J. Mater. Res. Technol. 8 (2019) 3800–3810.
[27] W. Rudzinski, W. Plazinski, Theoretical description of the kinetics of solute adsorption at heterogeneous solid/solution interfaces: on the possibility of distinguishing between the diffusional and the surface reaction kinetics models, Appl. Surf. Sci. 253 (2007) 5827–5840.
[28] H. Kızıltaş, Production of highly effective adsorbent from tea waste, and its adsorption behaviors and characteristics for the removal of Rhodamine B, Int. J. Environ. Anal. Chem. 104 (2024) 1730–1749.
[29] M.A. Nazir, M.S. Bashir, M. Jamshaid, A. Anum, T. Najam, K. Shahzad, A. ur Rehman, Synthesis of porous secondary metal-doped MOFs for removal of Rhodamine B from water: role of secondary metal on efficiency and kinetics, Surface. Interfac. 25 (2021) 101261.
[30] L. Peng, P. Qin, M. Lei, Q. Zeng, H. Song, J. Yang, J. Gu, Modifying Fe_3O_4 nanoparticles with humic acid for removal of Rhodamine B in water, J. Hazard Mater. 209 (2012) 193–198.
[31] H. Saufi, M.E. Alouani, J. Aride, M.H. Taibi, Rhodamine B biosorption from aqueous solution using Eichhornia crassipes powders: isotherm, kinetic and thermodynamic studies, Chemical Data Collections 25 (2020) 100330.
[32] M. Koyuncu, A.R. Kul, Thermodynamics and adsorption studies of dye (rhodamine-B) onto natural diatomite, Physicochem. Probl. Miner. Process. 50 (2014) 631–643.
[33] B. Damiyine, A. Guenbour, R. Boussen, Adsorption of rhodamine B dye onto expanded perlite from aqueous solution: kinetics, equilibrium and thermodynamics, J. Mater. Environ. Sci. 8 (2017) 345–355.
[34] F. Sabermahani, N.M. Mahani, M. Noraldiny, Removal of thallium (I) by activated carbon prepared from apricot nucleus shell and modified with rhodamine B, Toxin Rev. 36 (2017) 154–160.
[35] G. Vijayakumar, C.K. Yoo, K.G.P. Elango, M. Dharmendirakumar, Adsorption characteristics of rhodamine B from aqueous solution onto baryte, Clean–Soil, Air, Water 38 (2010) 202–209.
[36] M.K. Dahri, M.R.R. Kooh, L.B. Lim, Remediation of rhodamine B dye from aqueous solution using Casuarina equisetifolia cone powder as a low-cost adsorbent, Advances in physical chemistry (2016) 9497378.
[37] D.L. Postai, C.A. Demarchi, F. Zanatta, D.C.C. Melo, C.A. Rodrigues, Adsorption of rhodamine B and methylene blue dyes using waste of seeds of Aleurites Moluccana, a lowcost adsorbent, Alex. Eng. J. 55 (2016) 1713–1723.
[38] R. Elmoubarki, F.Z. Mahjoubi, H. Tounsadi, J. Moustadraf, M. Abdennouri, A. Zouhri, A. Albani, N. Barka, Adsorption of textile dyes on raw and decanted Moroccan clays: kinetics, equilibrium and thermodynamics, Water Resour. Ind. 9 (2015) 16–29.
[39] B. Cetin, H.I. Unal, O. Erol, Synthesis, characterization, and electrokinetic properties of polyindene/colemanite conducting composite, Clay Clay Miner. 60 (2012) 300–314.
[40] A. Pal, A. Garain, D. Chowdhury, M.H. Mondal, B.A. Saha, Comparative spectral study on the interaction of organic dye Congo-red with selective aqueous micellar media of CPC, Rhamnolipids and Saponin, Tenside Surfactants Detergents 57 (2020) 401–407.
[41] C.C. Jimenez, A. Enríquez-Cabrera, O. González-Antonio, J. Ordóñez-Hernández, P.G. Lacroix, P. Labra-Vázquez, R. Santillan, State of the art of boron and tin complexes in second-and third-order nonlinear optics, Inorganics 6 (2018) 131.
[42] G.G. Hacıosmanoğlu, T. Doğruel, S. Genç, E.T. Oner, Z.S. Can, Adsorptive removal of bisphenol A from aqueous solutions using phosphonated levan, J. Hazard Mater. 374 (2019) 43–49.
[43] Y. Pavlyukevich, I. Levitskii, N. Mazura, Use of colemanite in glass fiber production, Glass Ceram. (2009) 66.
[44] G.G. Hacıosmanoğlu, M. Arenas, C. Mejías, J. Martín, J.L. Santos, I. Aparicio, E. Alonso, Adsorption of fluoroquinolone antibiotics from wáter and wastewater by colemanite, Int. J. Environ. Res. Publ. Health 20 (2023) 2646.
[45] J. Zhang, M.A. Gondal, W. Wei, T. Zhang, Q. Xu, K. Shen, Preparation of room temperature ferromagnetic $BiFeO_3$ and its application as an highly efficient magnetic separable adsorbent for removal of Rhodamine B from aqueous solution, J. Alloys Compd. 530 (2012) 107–110.
[46] M. Kizilca, M. Copur, Thermal dehydration of colemanite: kinetics and mechanism determined using the master plots method, Can. Metall. Q. 56 (2017) 259–271.